J. Fluid Mech. (1997), *vol.* 344, *pp.* 155–180. Printed in the United Kingdom

Analysis and modelling of anisotropies in the dissipation rate of turbulence

By CHARLES G. SPEZIALE[1] AND THOMAS B. GATSKI[2]

[1]Aerospace & Mechanical Engineering Department, Boston University, Boston, MA 02215, USA
[2]NASA Langley Research Center, Hampton, VA 23681, USA

(Received 20 October 1995 and in revised form 3 March 1997)

The modelling of anisotropies in the dissipation rate of turbulence is considered based on an analysis of the exact transport equation for the dissipation rate tensor. An algebraic model is systematically derived using integrity bases methods and tensor symmetry properties. The new model differs notably from all previously proposed models in that it depends nonlinearly on the mean velocity gradients. This gives rise to a transport equation for the scalar dissipation rate that is of the same general form as the commonly used model with one major exception: the coefficient of the production term is dependent on the invariants of both the rotational and irrotational strain rates. The relationship between the new model and other recently proposed models is examined in detail. Some basic tests and applications of the model are also provided along with a discussion of the implications for turbulence modelling.

1. Introduction

It is often asserted that the modelled dissipation rate equation which is used in conjunction with most Reynolds stress turbulence closures is without theoretical foundation and, as such, constitutes the weak link in these models. In the formulation of dissipation rate models, the Kolmogorov hypothesis of local isotropy is routinely invoked (cf. Hinze 1975). This hypothesis – which states that in the limit of infinite Reynolds numbers the nonlinear scrambling of the cascade process eradicates anisotropies in the small scales – is unproven and can be debated (see Durbin & Speziale 1991 and the contrasting views of Saddoughi & Veeravalli 1994). However, one fact is incontrovertible: the preponderance of results from physical and numerical experiments indicate that at low to moderate turbulence Reynolds numbers there can be large anisotropies in the dissipation rate. For example, physical and numerical experiments on homogeneous turbulence for Taylor-microscale-based Reynolds numbers R_λ in the range of 10–50 (see Tavoularis & Corrsin 1981 and Lee & Reynolds 1985), indicate that the anisotropies in the dissipation rate tensor are more than half as large as those in the Reynolds stress tensor and, therefore, cannot be neglected. Nevertheless, in the logarithmic region of a turbulent boundary layer – which starts at $y^+ = 30$ where $R_\lambda \approx 30$ – Reynolds stress turbulence closures that neglect anisotropies in the dissipation rate are routinely applied. This is just one example of the type of inconsistency that establishes the motivation for the present paper.

In this paper, an analysis and systematic derivation of a model for the anisotropic part of the dissipation rate tensor of turbulence will be presented. The starting

point will be the exact transport equation for the dissipation rate tensor, simplified to the case of homogeneous turbulence. It will then be closed by modelling the higher-order correlations based on two major considerations: exact tensor symmetry properties along with the assumption that the anisotropies in the dissipation rate are sufficiently small so that nonlinearities in these terms can be neglected. An implicit algebraic system of equations for the anisotropy of dissipation will then be obtained after the same type of local equilibrium hypothesis is invoked as that which gives rise to algebraic stress models (ASM) for the Reynolds stress tensor (see Pope 1975 and Gatski & Speziale 1993). The solution of this implicit algebraic system by integrity bases methods leads to a new algebraic model for the anisotropy of dissipation that differs from all previously proposed models in one notable way: it is *nonlinear* in the mean velocity gradients. Since the pressure–strain correlation depends linearly on the mean velocity gradients in homogeneous turbulence, this calls into question the commonly adopted practice of modelling together the pressure–strain correlation and deviatoric part of the dissipation rate tensor (cf. Lumley 1978).

The algebraic model to be obtained in this study for the anisotropic part of the dissipation rate will then be introduced into the contraction of the transport equation for the dissipation rate tensor, and will be developed for moderate to relatively high turbulence Reynolds numbers. This will lead to a more rigorously based modelled transport equation for the scalar dissipation rate that is of the same general form as the commonly used model with one notable exception: the coefficient of the production term depends nonlinearly on the invariants of both rotational and irrotational strain rates. A model containing a similar nonlinear dependence on irrotational strain rates was recently obtained by Yakhot *et al.* (1992) via a heuristic Padé approximation in an RNG-based $K-\varepsilon$ model. Comparisons will be made between the new model and other models containing more *ad hoc* strain-dependent corrections that have been proposed over the past two decades (Pope 1978; Hanjalic & Launder 1980; Lumley 1992). Some illustrative calculations of homogeneous turbulent flows will be presented in order to test the new model and to gain insight into the behaviour of previously proposed models. Two more complex applications will also be considered, where inhomogeneous effects are significant, including a wall-bounded flow.

2. Theoretical background

The turbulent flow of a viscous incompressible fluid will be considered that is governed by the Navier–Stokes and continuity equations which can be written in the form

$$\frac{\partial v_i}{\partial t} + v_j \frac{\partial v_i}{\partial x_j} = -\frac{\partial P}{\partial x_i} + \nu \nabla^2 v_i, \tag{1}$$

$$\frac{\partial v_i}{\partial x_i} = 0, \tag{2}$$

where the Einstein summation convention applies to repeated indices. In (1), v_i represents the velocity vector, P denotes the kinematic pressure and ν is the kinematic viscosity. The velocity and pressure are decomposed into ensemble mean and fluctuating parts, respectively, given by

$$v_i = \overline{v}_i + u_i, \quad P = \overline{P} + p, \tag{3}$$

where an overbar denotes an ensemble mean. The ensemble mean of (1)–(2) yields the Reynolds-averaged Navier–Stokes and continuity equations

$$\frac{\partial \overline{v}_i}{\partial t} + \overline{v}_j \frac{\partial \overline{v}_i}{\partial x_j} = -\frac{\partial \overline{P}}{\partial x_i} + \nu \nabla^2 \overline{v}_i - \frac{\partial \tau_{ij}}{\partial x_j}, \tag{4}$$

$$\frac{\partial \overline{v}_i}{\partial x_i} = 0, \tag{5}$$

where

$$\tau_{ij} \equiv \overline{u_i u_j} \tag{6}$$

is the Reynolds stress tensor.

For simplicity, we will base most of our analysis on homogeneous turbulence where all correlations that are built up from the fluctuating velocity and pressure are spatially uniform. Extensions to inhomogeneous turbulent flows will be discussed briefly in a later section. For homogeneous turbulence, the fluctuating velocity u_i is a solution of the transport equation

$$\frac{\partial u_i}{\partial t} + \overline{v}_j \frac{\partial u_i}{\partial x_j} = -u_j \frac{\partial u_i}{\partial x_j} - u_j \frac{\partial \overline{v}_i}{\partial x_j} - \frac{\partial p}{\partial x_i} + \nu \nabla^2 u_i \tag{7}$$

which is obtained by subtracting (4) from (1) after making use of the fact that $\partial \tau_{ij}/\partial x_j = 0$ by homogeneity. Of course, (7) is solved subject to the incompressibility constraint

$$\frac{\partial u_i}{\partial x_i} = 0 \tag{8}$$

obtained by subtracting (5) from (2). We can write (7) in the symbolic nonlinear operator form

$$\mathcal{N} u_i = 0. \tag{9}$$

Then, the second moment

$$\overline{u_i \mathcal{N} u_j + u_j \mathcal{N} u_i} = 0 \tag{10}$$

yields the Reynolds stress transport equation for homogeneous turbulence (cf. Hinze 1975)

$$\dot{\tau}_{ij} = -\tau_{ik} \frac{\partial \overline{v}_j}{\partial x_k} - \tau_{jk} \frac{\partial \overline{v}_i}{\partial x_k} + \Pi_{ij} - \varepsilon_{ij}. \tag{11}$$

In (11), Π_{ij} and ε_{ij} are, respectively, the pressure–strain correlation and dissipation rate tensor of turbulence defined by

$$\Pi_{ij} \equiv \overline{p \left(\frac{\partial u_i}{\partial x_j} + \frac{\partial u_j}{\partial x_i} \right)}, \tag{12}$$

$$\varepsilon_{ij} = 2\nu \overline{\frac{\partial u_i}{\partial x_k} \frac{\partial u_j}{\partial x_k}}. \tag{13}$$

Models are only needed for Π_{ij} and ε_{ij} in order to achieve a Reynolds stress closure for homogeneous turbulence.

An analysis of the Poisson equation for pressure yields (see Launder, Reece & Rodi 1975; Reynolds 1987)

$$\Pi_{ij} = A_{ij} + M_{ijkl} \frac{\partial \overline{v}_k}{\partial x_l} \tag{14}$$

where, for homogeneous turbulence, A_{ij} and M_{ijkl} are functionals of the energy

spectrum tensor. These terms are typically modelled algebraically in the form (see Lumley 1978; Reynolds 1987; Speziale 1991):

$$A_{ij} = \varepsilon \mathscr{A}_{ij}(\boldsymbol{b}), \tag{15}$$

$$M_{ijkl} = K \mathscr{M}_{ijkl}(\boldsymbol{b}), \tag{16}$$

where $K = \frac{1}{2}\tau_{ii}$ is the turbulent kinetic energy, $\varepsilon = \frac{1}{2}\varepsilon_{ii}$ is the scalar turbulent dissipation rate and

$$b_{ij} = \frac{\tau_{ij} - \frac{2}{3}K\delta_{ij}}{2K} \tag{17}$$

is the Reynolds stress anisotropy tensor. The representations (15)–(16) are only rigorously justified for homogeneous turbulent flows that are near equilibrium (see Speziale 1996).

A transport equation for the dissipation rate tensor can be obtained by constructing the moment

$$\overline{2\nu \frac{\partial u_i}{\partial x_k}\frac{\partial}{\partial x_k}(\mathscr{N} u_j) + 2\nu \frac{\partial u_j}{\partial x_k}\frac{\partial}{\partial x_k}(\mathscr{N} u_i)} = 0. \tag{18}$$

For homogeneous turbulence this exact transport equation takes the form (see Durbin & Speziale 1991)

$$\dot{\varepsilon}_{ij} = -\varepsilon_{ik}\frac{\partial \overline{v}_j}{\partial x_k} - \varepsilon_{jk}\frac{\partial \overline{v}_i}{\partial x_k} + 2(f_{ikjl} + f_{jkil} - f_{lkij})\frac{\partial \overline{v}_k}{\partial x_l} + N_{ij}, \tag{19}$$

where

$$f_{ijkl} \equiv 2\nu \overline{\frac{\partial u_k}{\partial x_i}\frac{\partial u_l}{\partial x_j}}, \tag{20}$$

$$N_{ij} \equiv 2\nu \overline{\left(\frac{\partial u_i}{\partial x_j} + \frac{\partial u_j}{\partial x_i}\right)\frac{\partial u_l}{\partial x_k}\frac{\partial u_k}{\partial x_l}} - 2\nu \overline{\frac{\partial u_i}{\partial x_l}\frac{\partial u_k}{\partial x_l}\frac{\partial u_j}{\partial x_k}} - 2\nu \overline{\frac{\partial u_j}{\partial x_l}\frac{\partial u_k}{\partial x_l}\frac{\partial u_i}{\partial x_k}} - 4\nu^2 \overline{\frac{\partial^2 u_i}{\partial x_k \partial x_l}\frac{\partial^2 u_j}{\partial x_k \partial x_l}}. \tag{21}$$

In most Reynolds stress turbulence closures, the Kolmogorov hypothesis of local isotropy is invoked whereby it is assumed that (cf. Hinze 1975)

$$\varepsilon_{ij} = \tfrac{2}{3}\varepsilon\delta_{ij}. \tag{22}$$

A modelled version of the contraction of the transport equation (19) is then solved. This equation, which typically takes the form (see Launder *et al.* 1975)

$$\dot{\varepsilon} = -C_{\varepsilon 1}\frac{\varepsilon}{K}\tau_{ij}\frac{\partial \overline{v}_i}{\partial x_j} - C_{\varepsilon 2}\frac{\varepsilon^2}{K} \tag{23}$$

in homogeneous turbulence (where $C_{\varepsilon 1}$ and $C_{\varepsilon 2}$ are constants), is usually postulated in an *ad hoc* manner. The primary purpose of this paper, as elucidated earlier, is to provide a more systematic treatment of the dissipation rate equation where anisotropies in the dissipation are accounted for.

3. Anisotropic dissipation rate model

Our analysis begins with the exact transport equation for the dissipation rate tensor given by (19)–(21). In order to achieve closure, models are needed for f_{ijkl} and N_{ij}.

The correlation f_{ijkl}, which is a fourth-rank tensor, has a variety of symmetry and normalization properties which can be listed as follows (see Durbin & Speziale 1991):

$$f_{ijkl} = f_{jikl} = f_{ijlk}, \tag{24}$$

$$f_{ijil} = f_{ilkl} = f_{ikkl} = f_{ljkl} = 0, \tag{25}$$

$$f_{iikl} = \varepsilon_{kl}, \quad f_{ijkk} = \varepsilon_{ij}^{(c)}, \tag{26}$$

where

$$\varepsilon_{ij}^{(c)} = 2\nu \overline{\frac{\partial u_k}{\partial x_i} \frac{\partial u_k}{\partial x_j}} \tag{27}$$

is the complementary dissipation rate tensor which constitutes a type of 'structure' tensor since it contains information on the dimensionality of the turbulence (the third invariant of $\varepsilon_{ij}^{(c)}$ vanishes for two-dimensional turbulence). Here, (24) follows from homogeneity and the interchangeability of the order of differentiation, (25) follows directly from the continuity equation and (26) from the definition of ε_{ij} and $\varepsilon_{ij}^{(c)}$. Durbin & Speziale (1991) showed that if local isotropy applies, then

$$f_{ijkl}^{*} = \tfrac{4}{15}\delta_{ij}\delta_{kl} - \tfrac{1}{15}(\delta_{ik}\delta_{jl} + \delta_{jk}\delta_{il}) \tag{28}$$

where $f_{ijkl}^{*} \equiv \frac{1}{\varepsilon} f_{ijkl}$ is a non-dimensional tensor.

The anisotropy of dissipation is characterized by the dimensionless tensor

$$d_{ij} = \frac{\varepsilon_{ij} - \frac{2}{3}\varepsilon\delta_{ij}}{2\varepsilon}. \tag{29}$$

Similarly, the anisotropy of the complementary dissipation is defined as

$$d_{ij}^{(c)} = \frac{\varepsilon_{ij}^{(c)} - \frac{2}{3}\varepsilon\delta_{ij}}{2\varepsilon}. \tag{30}$$

As with the Reynolds stress anisotropy tensor b_{ij}, both d_{ij} and $d_{ij}^{(c)}$ have eigenvalues that lie between $-\frac{1}{3}$ and $\frac{2}{3}$. In uniformly sheared and strained turbulent flows, there is a wealth of evidence from physical and numerical experiments which suggests that a structural equilibrium is ultimately reached where b_{ij} and d_{ij} – as well as all appropriately normalized higher-order correlations – achieve constant values (cf. Tavoularis & Corrsin 1981 and Rogers, Moin & Reynolds 1986).

We propose to describe departures from local isotropy by the form

$$f_{ijkl}^{*} = f_{ijkl}^{*}(d_{mn}) \tag{31}$$

where $f_{ijkl}^{*}(0)$ is given by (28) (when $d_{mn} = 0$, (31) reduces to the isotropic form). For basic homogeneous turbulent flows, such as uniform shear flow, that are near equilibrium,

$$\|\boldsymbol{d}\| \sim O(10^{-1}) \tag{32}$$

(see Tavoularis & Corrsin 1981 and Rogers *et al.* 1986). Hence, it appears that a linear approximation to (31) should be adequate. The most general linear form for (31) that is tensorially invariant is given by

$$\begin{aligned} f_{ijkl}^{*} = {} & \alpha_0\delta_{ij}\delta_{kl} + \alpha_1(\delta_{ik}\delta_{jl} + \delta_{il}\delta_{jk}) \\ & + \alpha_2\delta_{ij}d_{kl} + \alpha_3\delta_{kl}d_{ij} + \alpha_4(\delta_{ik}d_{jl} + \delta_{jk}d_{il} + \delta_{il}d_{jk} + \delta_{jl}d_{ik}) \end{aligned} \tag{33}$$

where $\alpha_0 - \alpha_4$ are constants. After applying the symmetry and normalization con-

straints (24)–(26), the general linear representation (33) simplifies to

$$f^*_{ijkl} = \tfrac{4}{15}\delta_{ij}\delta_{kl} - \tfrac{1}{15}(\delta_{ik}\delta_{jl} + \delta_{jk}\delta_{il}) + \left(\tfrac{4}{11}\alpha_3 + \tfrac{10}{11}\right)\delta_{ij}d_{kl} + \alpha_3\delta_{kl}d_{ij} - \left(\tfrac{3}{11}\alpha_3 + \tfrac{2}{11}\right)(\delta_{ik}d_{jl} + \delta_{jk}d_{il} + \delta_{il}d_{jk} + \delta_{jl}d_{ik}) \tag{34}$$

where α_3 is a yet undetermined constant. From the second normalization constraint (26), it follows that

$$d^{(c)}_{ij} = \tfrac{1}{2}\left(\tfrac{21}{11}\alpha_3 - \tfrac{8}{11}\right)d_{ij}. \tag{35}$$

Equation (35) implies that $d^{(c)}_{ij} \propto d_{ij}$; this has some support from DNS results for simple turbulent shear flows (cf. Rogers *et al.* 1986). These DNS results indirectly suggest that $\alpha_3 \approx 0.6$ – a point that will be discussed in more detail later.

Closure of the transport equation (19) for the turbulent dissipation rate tensor is achieved once a model is provided for the correlation N_{ij} which encompasses the effects of vortex stretching and viscous diffusion. We decompose N_{ij} into isotropic and deviatoric parts as follows:

$$N_{ij} = \tfrac{2}{3}N\delta_{ij} + {}_DN_{ij} \tag{36}$$

where $N \equiv \frac{1}{2}N_{ii}$. The isotropic part of (36) is usually modelled in the classical form

$$N = C_{\varepsilon 1}\frac{\varepsilon}{K}\mathscr{P} - C_{\varepsilon 2}\frac{\varepsilon^2}{K} \tag{37}$$

where $\mathscr{P} \equiv -\tau_{ij}\partial\bar{v}_i/\partial x_j$ is the turbulence production and $C_{\varepsilon 1}$ and $C_{\varepsilon 2}$ are constants in equilibrium. This will be discussed in more detail later. When local isotropy is invoked, (34), (36) and (37) yield the classical modelled transport equation (cf. Lumley 1978 and Speziale 1991)

$$\dot{\varepsilon} = C_{\varepsilon 1}\frac{\varepsilon}{K}\mathscr{P} - C_{\varepsilon 2}\frac{\varepsilon^2}{K}. \tag{38}$$

It should be remembered that when local isotropy is assumed,

$$\varepsilon_{ij} = \tfrac{2}{3}\varepsilon\delta_{ij}, \quad N_{ij} = \tfrac{2}{3}N\delta_{ij} \tag{39}$$

and

$$f_{ijkl} = \tfrac{4}{15}\varepsilon\delta_{ij}\delta_{kl} - \tfrac{1}{15}\varepsilon(\delta_{ik}\delta_{jl} + \delta_{jk}\delta_{il}) \tag{40}$$

which reduces the trace of (19) to (38) given that (37) is valid.

For homogeneous turbulence, the turbulent kinetic energy K is a solution of the exact transport equation

$$\dot{K} = \mathscr{P} - \varepsilon \tag{41}$$

which follows from a contraction of (11) since Π_{ij} is traceless. From (38) and (41), it follows that the inverse of the turbulent time scale ε/K satisfies the transport equation

$$\frac{\mathrm{d}}{\mathrm{d}t}\left(\frac{\varepsilon}{K}\right) = \left[(C_{\varepsilon 1} - 1)\frac{\mathscr{P}}{\varepsilon} - (C_{\varepsilon 2} - 1)\right]\frac{\varepsilon^2}{K^2}. \tag{42}$$

For isotropic turbulence, where $\mathscr{P} = 0$, (42) renders $\varepsilon/K \to 0$ as $t \to \infty$ (i.e. the turbulent time scale K/ε grows monotonically according to a linear power law). In the limit in which local isotropy holds exactly for a turbulent flow which is anisotropic at the large scales, there should be a complete decoupling of the large scales from the small scales through nonlinear scrambling. Then, as with the case of isotropic

turbulence, it could be hypothesized that the turbulent time scale should also grow monotonically in an anologous way, becoming infinite in the limit as $t \to \infty$. Unless $C_{\varepsilon 1} = 1$, K/ε goes to a finite fixed point (see Speziale 1990). Hence, we hypothesize that

$$C_{\varepsilon 1} = 1 \tag{43}$$

for full consistency with the limit of local isotropy. The constant $C_{\varepsilon 2}$ can be evaluated from the decay of isotropic turbulence. Equation (38) renders the long-time asymptotic power law decay

$$K \sim t^{-1/(C_{\varepsilon 2}-1)} \tag{44}$$

where $C_{\varepsilon 2} \approx 1.83$ based on the average of the isotropic decay experiments of Comte-Bellot & Corrsin (1971).

The principal role of the deviatoric part of N_{ij} is to generate a return to isotropy in the absence of mean straining. For example, the homogeneous experiments of Maréchal (1972) indicate that at moderate turbulence Reynolds numbers, mean straining can induce significant anisotropies in the small scales. However, when the straining is removed, the small scales rapidly return to isotropy. In the absence of mean velocity gradients, (19) implies that

$$_D\dot{\varepsilon}_{ij} = {}_DN_{ij} \tag{45}$$

where ${}_D\varepsilon_{ij}$ represents the deviatoric part of the dissipation rate tensor. The return to isotropy can be described by the simple relaxation model

$$_D\dot{\varepsilon}_{ij} = -\frac{C_{\varepsilon 5}}{T}{}_D\varepsilon_{ij} \tag{46}$$

where $C_{\varepsilon 5}$ is a constant and T is an appropriate time scale. Equation (46) is analogous to the Rotta return to isotropy model used in the Reynolds stress transport equation. There is some question as to what is the proper choice of the time scale T. One may be tempted to pick the Kolmogorov time scale $(\nu/\varepsilon)^{1/2}$. However, then

$$\frac{1}{T} = R_t^{1/2}\frac{\varepsilon}{K}$$

(where $R_t \equiv K^2/\nu\varepsilon$ is the turbulence Reynolds number) which would imply that $1/T \to \infty$ as $R_t \to \infty$. This is a highly questionable result in that it suggests that at moderately high turbulence Reynolds numbers there would virtually be an instantaneous return to isotropy. This is not consistent with the most recent experiments which indicate non-negligible small-scale anisotropy at relatively high turbulence Reynolds numbers (see Sreenivasan 1991). Hence, the time scale T is probably a more complex combination of the Kolmogorov time scale $(\nu/\varepsilon)^{1/2}$ and the turbulent time scale (K/ε). This then leads to a model of the form

$$_DN_{ij} = -C_{\varepsilon 5}\frac{\varepsilon}{K}\left(\varepsilon_{ij} - \tfrac{2}{3}\varepsilon\delta_{ij}\right) \tag{47}$$

where

$$C_{\varepsilon 5} = C_{\varepsilon 5}(R_t). \tag{48}$$

If one accepts the Kolmogorov hypothesis of local isotropy, then $C_{\varepsilon 5} \to \infty$ as $R_t \to \infty$. However, as alluded to earlier, the recent experiments of Sreenivasan (1991) tend to indicate that astronomically large turbulence Reynolds numbers may be needed for local isotropy to be valid in a strong approximate sense (Durbin & Speziale 1991 raised questions as to whether significantly strained turbulent flows ever become

isotropic at the small scales even in the limit as $R_t \to \infty$). Consequently, for the turbulence Reynolds numbers encountered in practical flows – which are usually at most only moderately high – $C_{\varepsilon 5}$ can be approximated as a constant. Then, the relaxational experiments of Maréchal (1972) on the return to isotropy of the small scales indicate that

$$C_{\varepsilon 5} \approx 5.0 \tag{49}$$

as first determined by P. Durbin (private communication) by a comparison of the experimental rate at which the small scales return to isotropy with the analytical solution to (46). Calculations have indicated that a value of 5.80 works best with the overall model presented herein as will soon be explained.

We now have closure of the homogeneous dissipation rate transport equation (19). This modelled transport equation takes the form

$$\begin{aligned}\dot{\varepsilon}_{ij} = &-\varepsilon_{ik}\frac{\partial \overline{v}_j}{\partial x_k} - \varepsilon_{jk}\frac{\partial \overline{v}_i}{\partial x_k} + \tfrac{16}{15}\varepsilon \overline{S}_{ij} \\ &+ \left(\tfrac{30}{11}\alpha_3 + \tfrac{20}{11}\right)\varepsilon(d_{ik}\overline{S}_{jk} + d_{jk}\overline{S}_{ik} - \tfrac{2}{3}d_{kl}\overline{S}_{kl}\delta_{ij}) - \left(\tfrac{14}{11}\alpha_3 - \tfrac{20}{11}\right)\varepsilon(d_{ik}\overline{W}_{jk} + d_{jk}\overline{W}_{ik}) \\ &- \left(\tfrac{14}{11}\alpha_3 - \tfrac{16}{33}\right)\varepsilon d_{kl}\overline{S}_{kl}\delta_{ij} + \frac{2}{3}\left(C_{\varepsilon 1}\frac{\varepsilon}{K}\mathscr{P} - C_{\varepsilon 2}\frac{\varepsilon^2}{K}\right)\delta_{ij} - C_{\varepsilon 5}\frac{\varepsilon}{K}\left(\varepsilon_{ij} - \tfrac{2}{3}\varepsilon\delta_{ij}\right)\end{aligned} \tag{50}$$

where

$$\overline{S}_{ij} = \frac{1}{2}\left(\frac{\partial \overline{v}_i}{\partial x_j} + \frac{\partial \overline{v}_j}{\partial x_i}\right), \quad \overline{W}_{ij} = \frac{1}{2}\left(\frac{\partial \overline{v}_i}{\partial x_j} - \frac{\partial \overline{v}_j}{\partial x_i}\right) \tag{51}$$

are the mean rate of strain and mean vorticity tensors. Equation (50) is obtained by substituting (34), (37) and (47) into (19). The striking thing about this model is that it contains only two additional constants over those which appear in the traditional modelled scalar dissipation rate equation. As mentioned before, the constants α_3 and $C_{\varepsilon 5}$ have been determined to take the approximate values of 0.6 and 5.80, respectively. This was accomplished by using the DNS data of Rogers *et al.* (1986) for homogeneous shear flow and the relaxational experiments of Maréchal (1972) along with other physical constraints to be discussed later. The results of Rogers *et al.* (1986) for homogeneous shear flow indicate that the equilibrium value of the shear component of the anisotropy of dissipation is given by

$$d_{12} \approx -0.06$$

to within, at most, a 3% deviation in their three best-resolved runs. This is the most important component since it is the only contributor to the production of dissipation. On the other hand, the normal components of d_{ij} exhibit as much as a 50% deviation between runs making them unsuitable for purposes of model calibration. With the choice of constants $\alpha_3 = 0.6$ and $C_{\varepsilon 5} = 5.80$ we predict the equilibrium value

$$d_{12} = -0.057$$

in homogeneous shear flow with the most energetic growth rate in rotating homogeneous shear flow correctly placed at $\Omega/S = 0.25$ – without enforcing Richardson number similarity which is known to be violated – overcoming an earlier deficiency in second-order closures (see Speziale, Sarkar & Gatski 1991 for more details).

Two different approaches can be pursued at this point for more general turbulent flows: (*a*) turbulent diffusion terms can be added to the right-hand side of (50) via a gradient transport hypothesis or (*b*) an algebraic model can be obtained from (50) by invoking a local homogeneous equilibrium hypothesis. Since the former approach

requires the solution of an additional five transport equations in three dimensions – along with the added complication of providing boundary conditions for each component of the dissipation rate tensor which may be infeasible in many flow situations – we will pursue the latter approach which appears to be more practical for complex flows.

For homogeneous turbulent flows in equilibrium,

$$\frac{\mathrm{d}}{\mathrm{d}t}(d_{ij}) = 0, \quad \frac{\mathrm{d}}{\mathrm{d}t}\left(\frac{\varepsilon}{K}\right) = 0 \tag{52}$$

since all structural quantities achieve constant values that are largely independent of the initial conditions in the limit as $t \to \infty$ (the same is true of b_{ij} and $d_{ij}^{(c)}$). Equation (52) implies that

$$\frac{\dot{\varepsilon}_{ij}}{2\varepsilon} - \frac{\varepsilon_{ij}}{2\varepsilon^2}\dot{\varepsilon} = 0, \quad \frac{\dot{\varepsilon}}{K} - \frac{\varepsilon}{K^2}\dot{K} = 0 \tag{53}$$

and, hence, after (41) is made use of, we have

$$\dot{\varepsilon}_{ij} = \frac{\varepsilon}{K}\left(\frac{\mathscr{P}}{\varepsilon} - 1\right)\varepsilon_{ij} \tag{54}$$

in equilibrium. The substitution of (54) into (50) yields the linear algebraic system of equations

$$\begin{aligned}\frac{\varepsilon}{K}\left(\frac{\mathscr{P}}{\varepsilon} - 1\right) d_{ij} = &-d_{ik}\frac{\partial \overline{v}_j}{\partial x_k} - d_{jk}\frac{\partial \overline{v}_i}{\partial x_k} + \frac{2}{3}d_{kl}\overline{S}_{kl}\delta_{ij} - C_{\varepsilon 5}\frac{\varepsilon}{K}d_{ij} \\ &-\tfrac{2}{15}\overline{S}_{ij} + \left(\tfrac{15}{11}\alpha_3 + \tfrac{10}{11}\right)\left(d_{ik}\overline{S}_{jk} + d_{jk}\overline{S}_{ik} - \tfrac{2}{3}d_{kl}\overline{S}_{kl}\delta_{ij}\right) \\ &-\left(\tfrac{7}{11}\alpha_3 - \tfrac{10}{11}\right)(d_{ik}\overline{W}_{jk} + d_{jk}\overline{W}_{ik}).\end{aligned} \tag{55}$$

In obtaining (55) we have made use of the fact that

$$(C_{\varepsilon 1} - 1)\frac{\mathscr{P}}{K} - (C_{\varepsilon 2} - 1)\frac{\varepsilon}{K} - \left(\tfrac{21}{11}\alpha_3 + \tfrac{14}{11}\right) d_{kl}\overline{S}_{kl} = 0 \tag{56}$$

in equilibrium which follows from (38), (41), (42) and (53).

The linear system (55) can be solved by integrity bases techniques; this is completely analogous to the way algebraic stress models are obtained from the Reynolds stress transport equation (see Pope 1975 and Gatski & Speziale 1993). For two-dimensional mean velocity gradients – which tend to generate the largest anisotropy – the solution of (55) is given by (see the Appendix)

$$\begin{aligned}d_{ij} = -2C_{\mu\varepsilon}\Bigg[&\frac{K}{\varepsilon}\overline{S}_{ij} + \left(\frac{\frac{7}{11}\alpha_3 + \frac{1}{11}}{C_{\varepsilon 5} + \mathscr{P}/\varepsilon - 1}\right)\frac{K^2}{\varepsilon^2}(\overline{S}_{ik}\overline{W}_{kj} + \overline{S}_{jk}\overline{W}_{ki}) \\ &+ \left(\frac{\frac{30}{11}\alpha_3 - \frac{2}{11}}{C_{\varepsilon 5} + \mathscr{P}/\varepsilon - 1}\right)\frac{K^2}{\varepsilon^2}\left(\overline{S}_{ik}\overline{S}_{kj} - \tfrac{1}{3}\overline{S}_{kl}\overline{S}_{kl}\delta_{ij}\right)\Bigg]\end{aligned} \tag{57}$$

where

$$C_{\mu\varepsilon} = \frac{1}{15(C_{\varepsilon 5} + \mathscr{P}/\varepsilon - 1)}\left[1 + 2\left(\frac{\frac{7}{11}\alpha_3 + \frac{1}{11}}{C_{\varepsilon 5} + \mathscr{P}/\varepsilon - 1}\right)^2 \xi^2 - \frac{2}{3}\left(\frac{\frac{15}{11}\alpha_3 - \frac{1}{11}}{C_{\varepsilon 5} + \mathscr{P}/\varepsilon - 1}\right)^2 \eta^2\right]^{-1}, \tag{58}$$

Case	Rogallo (1981)	ADRM
$BSH9U$	-0.064	-0.056
$BSH11K$	-0.063	-0.056
$BSH12R$	-0.064	-0.056

TABLE 1. A comparison of the predictions of the ADRM(57) for d_{12} with results from Rogallo (1981).

$$\eta = (\overline{S}_{ij}\overline{S}_{ij})^{1/2}\frac{K}{\varepsilon}, \quad \xi = (\overline{W}_{ij}\overline{W}_{ij})^{1/2}\frac{K}{\varepsilon}. \tag{59}$$

For three-dimensional mean velocity gradients, the solution to (55) is much more complicated; it contains nine terms rather than three (it is of the same tensorial form as the three-dimensional algebraic stress model; see Gatski & Speziale 1993). However, for three-dimensional strain-dominated flows, (57) represents an excellent approximation; furthermore, for the general three-dimensional case, (57) still constitutes the leading-order terms. On this basis, we propose to use (57) for simplicity.

The key feature that distinguishes (57) from all previously proposed algebraic models for the anisotropy of dissipation is that it is *nonlinear* in the mean velocity gradients. Previously proposed algebraic models have, for the most part, been parameterized in terms of the Reynolds stress anisotropy tensor b_{ij} – a point to be discussed later (cf. Lumley 1978; Hallbäck, Groth & Johansson 1990; Lee & Reynolds 1985). Another interesting point is the way that $C_{\varepsilon 5}$ appears in (57)–(58). Consistent with the limit of local isotropy, $d_{ij} \to 0$ as $C_{\varepsilon 5} \to \infty$ as mentioned earlier. Since the dissipation equilibrates on a much faster time scale than the Reynolds stress tensor, we believe that an algebraic model has the potential to be successful under a fairly wide range of circumstances.

It is our purpose to develop a model that is suitable for use in practical turbulent flows that have moderate to relatively high turbulence Reynolds numbers. One of the few existing DNS databases that fits this category is that for homogeneous shear flow. Since homogeneous shear flow allows computations to be done for a longer elapsed time – and since the turbulent kinetic energy and, hence, the turbulence Reynolds number grow exponentially – moderately large turbulence Reynolds numbers are achieved by the conclusion of these runs unlike in plane strain, the axisymmetric expansion/contracton or relaxational turbulent flows. Thus, as explained herein, we came to the conclusion that homogeneous shear flow was the only useful DNS database for the purposes of quantitative comparisons. Since the results of Rogers *et al.* (1986) were used for the model calibration, it would be useful to also check the model with the DNS results of Rogallo (1981). A comparison of the predictions of the new algebraic anisotropic dissipation rate model (ADRM) for d_{12} are compared in table 1 with the final values taken from three of the runs of Rogallo (1981) for homogeneous shear flow. It is clear that these results are in line with those of Rogers *et al.* (1986) and that the new model does a good job in capturing the crucial shear component of the dissipation rate anisotropy tensor. As with the DNS results of Rogers *et al.* (1986), we do not compare with the normal components of d_{ij} since the data exhibit more than a 50% spread in the results between runs. The new algebraic model for the dissipation rate anisotropy will be analysed more extensively in the Sections to follow.

4. The scalar dissipation rate equation

In this Section, a more systematic analysis of the scalar dissipation rate equation will be presented which accounts for the effects of anisotropic dissipation. The algebraic model (57) will be relied on heavily. From the contraction of (19), it follows that

$$\dot{\varepsilon} = -2\varepsilon(d_{ij} + d_{ij}^{(c)})\,\frac{\partial \overline{v}_i}{\partial x_j} - 2\nu\,\overline{\frac{\partial u_i \partial u_i \partial u_k}{\partial x_k \partial x_l \partial x_l}} - 2\nu^2\,\overline{\frac{\partial^2 u_i}{\partial x_k \partial x_l}\frac{\partial^2 u_i}{\partial x_k \partial x_l}} \tag{60}$$

where it should be noted that

$$N \equiv -2\nu\,\overline{\frac{\partial u_i}{\partial x_k}\frac{\partial u_i}{\partial x_l}\frac{\partial u_k}{\partial x_l}} - 2\nu^2\,\overline{\frac{\partial^2 u_i}{\partial x_k \partial x_l}\frac{\partial^2 u_i}{\partial x_k \partial x_l}}. \tag{61}$$

The first term on the right-hand side of (61) represents the production of dissipation by vortex stretching whereas the second term represents the destruction of dissipation by viscous diffusion. For isotropic turbulence,

$$-2\nu\,\overline{\frac{\partial u_i}{\partial x_k}\frac{\partial u_i}{\partial x_l}\frac{\partial u_k}{\partial x_l}} = \frac{7}{3\sqrt{15}} S_K\, R_t^{1/2}\,\frac{\varepsilon^2}{K} \tag{62}$$

where S_K is the velocity derivative skewness (cf. Speziale & Bernard 1992). The destruction of dissipation is of the form (cf. Speziale & Bernard 1992)

$$2\nu^2\,\overline{\frac{\partial^2 u_i}{\partial x_j \partial x_k}\frac{\partial^2 u_i}{\partial x_j \partial x_k}} = \frac{7}{3\sqrt{15}}\, G_K R_t^{1/2}\,\frac{\varepsilon^2}{K} + O\left(\frac{\varepsilon^2}{K}\right) \tag{63}$$

where G_K is a palinstrophy coefficient. Typically, an equilibrium hypothesis is invoked whereby it is assumed that

$$S_K = G_K. \tag{64}$$

This guarantees that the turbulence evolves on the turbulent time scale rather than on the Kolmogorov time scale which, at high Reynolds numbers, would constitute rapid changes characteristic of a highly non-equilibrium state. This is also in keeping with the traditional approach of modelling the dissipation as that which arises from the energy cascade which allows us to parametrize quantities in terms of large-scale fields. Hence, for isotropic turbulence in equilibrium at high Reynolds numbers,

$$N = -C_{\varepsilon 2}\frac{\varepsilon^2}{K} \tag{65}$$

where $C_{\varepsilon 2}$ is a constant. In anisotropic turbulent flows, (65) is extended as follows:

$$N = -C_{\varepsilon 2}\frac{\varepsilon^2}{K} - N^*\left(b_{ij}, \frac{\partial \overline{v}_i}{\partial x_j}, K, \varepsilon\right) \tag{66}$$

where $N^* \to 0$ as b_{ij} and $\partial \overline{v}_i/\partial x_j \to 0$. For small b_{ij}, a first-order Taylor expansion of N^*, subject to dimensional invariance, yields the result

$$N = -C_{\varepsilon 2}\frac{\varepsilon^2}{K} - 2C_{\varepsilon 1} b_{ij}\frac{\partial \overline{v}_i}{\partial x_j}\varepsilon \tag{67}$$

where $C_{\varepsilon 1}$ is a constant. Upon substituting the definition of b_{ij}, we arrive at (37) discussed in §3.

As mentioned earlier, if in the limit of local isotropy the small scales are to completely decouple from the large scales, it can be hypothesized that $C_{\varepsilon 1} = 1$. In equilibrium, the coefficient $C_{\varepsilon 2}$ is a constant at high Reynolds numbers; in the

isotropic limit, $C_{\varepsilon 2}$ must be in the range of 1.70 to 2.0 to collapse the decay rates of existing experiments.

By making use of (35) and (37), it follows that (60) takes the form

$$\dot{\varepsilon} = C_{\varepsilon 1}\frac{\varepsilon}{K}\mathscr{P} - 2(1+\alpha)\,\varepsilon d_{ij}\overline{S}_{ij} - C_{\varepsilon 2}\frac{\varepsilon^2}{K} \tag{68}$$

where

$$\alpha = \tfrac{3}{4}\left(\tfrac{14}{11}\alpha_3 - \tfrac{16}{33}\right). \tag{69}$$

When (57) and (68) are solved with the Reynolds stress transport equation (11) – and a model for the pressure–strain correlation is provided as will be discussed later – a complete Reynolds stress closure for homogeneous turbulence is achieved.

Equation (68) accounts for the direct effect of anisotropies in the dissipation on the scalar turbulent dissipation rate. It is to be used with the algebraic model (57) derived in §3 when implemented in the context of a full Reynolds stress closure based on the solution of (11). However, a more convenient form can be obtained that is suitable for use with two-equation turbulence models. For homogeneous mean turbulent flows that are two-dimensional and in equilibrium, second-order closures yield the Reynolds stress tensor (see Gatski & Speziale 1993)

$$\tau_{ij} = \tfrac{2}{3}K\delta_{ij} - \frac{1}{1-\gamma_1^2\eta^2+\gamma_2^2\xi^2}\left[2C_\mu\frac{K^2}{\varepsilon}\overline{S}_{ij} + \gamma_3\frac{K^3}{\varepsilon^2}(\overline{S}_{ik}\overline{W}_{kj} + \overline{S}_{jk}\overline{W}_{kj}) - \gamma_4\frac{K^3}{\varepsilon^2}\left(\overline{S}_{ik}\overline{S}_{kj} - \tfrac{1}{3}\overline{S}_{kl}\overline{S}_{kl}\delta_{ij}\right)\right] \tag{70}$$

where C_μ and $\gamma_1 - \gamma_4$ are constants. This form constitutes an excellent approximation for turbulent flows that have mild departures from equilibrium and mild to moderate three-dimensional effects provided that they are strain dominated. For such flows, (70) yields

$$\frac{\mathscr{P}}{\varepsilon} = 2C_\mu^*\eta^2 \tag{71}$$

where

$$C_\mu^* \equiv \frac{C_\mu}{1-\gamma_1^2\eta^2+\gamma_2^2\xi^2}. \tag{72}$$

Substituting (57) into (68) – after making use of (58), (59), (71) and (72) – yields

$$\dot{\varepsilon} = C_{\varepsilon 1}^*\frac{\varepsilon}{K}\mathscr{P} - C_{\varepsilon 2}\frac{\varepsilon^2}{K} \tag{73}$$

where

$$C_{\varepsilon 1}^* = C_{\varepsilon 1} + \frac{2(1+\alpha)}{15C_\mu^*}\left[\frac{C_{\varepsilon 5}+2C_\mu^*\eta^2-1}{(C_{\varepsilon 5}+2C_\mu^*\eta^2-1)^2 - \tfrac{2}{3}\beta_2^2\eta^2 + 2\beta_1^2\xi^2}\right] \tag{74}$$

and

$$\beta_1 \equiv \tfrac{7}{11}\alpha_3 + \tfrac{1}{11}, \quad \beta_2 \equiv \tfrac{15}{11}\alpha_3 - \tfrac{1}{11}. \tag{75}$$

In practical applications, C_μ^* can be approximated by its equilibrium value of $C_\mu^* \approx 0.094$ for shear flow. It is clear that we have $C_{\varepsilon 1}^* = C_{\varepsilon 1}^*(\eta, \xi)$. The physical consequences of this dependence will be discussed in the next Section.

Finally, to conclude this Section, some comments are in order concerning inhomogeneous and non-inertial effects. For both the complete algebraic dissipation rate

model and its simplified equilibrium form, the scalar dissipation rate equation can be written in the form

$$\dot{\varepsilon} = \mathscr{P}_\varepsilon - C_{\varepsilon 2}\frac{\varepsilon^2}{K} \tag{76}$$

in homogeneous turbulence where the production term $\mathscr{P}_\varepsilon$ is given either by the first two terms on the right-hand side of (68) or by the first term on the right-hand side of (73). It can be extended to inhomogeneous turbulent flows by the addition of turbulent diffusion terms which can be modelled via the standard gradient transport hypothesis (cf. Speziale 1991). This yields the following transport equation:

$$\frac{\partial \varepsilon}{\partial t} + \overline{v}_i\frac{\partial \varepsilon}{\partial x_i} = \mathscr{P}_\varepsilon - C_{\varepsilon 2}\frac{\varepsilon^2}{K} + C_\varepsilon\frac{\partial}{\partial x_i}\left(\frac{K}{\varepsilon}\tau_{ij}\frac{\partial \varepsilon}{\partial x_j}\right) \tag{77}$$

where C_ε is a constant that takes a value of approximately 0.15 in order to yield the correct von Kármán constant in boundary layers (see Launder *et al.* 1975). For inhomogeneous turbulent flows, the mean substantial derivative replaces the time derivative on the left-hand side of (76).

In non-inertial reference frames, Coriolis terms must be added to the right-hand side of (11) and (50). Furthermore, the mean vorticity tensor that appears in the pressure–strain model in (11), as well as on the right-hand side of (50), must be replaced with the absolute mean vorticity tensor

$$\overline{W}^*_{ij} = \overline{W}_{ij} + e_{mji}\Omega_m \tag{78}$$

where Ω_m is the angular velocity of the reference frame and e_{mji} is the permutation tensor. When these non-inertial effects are rigorously introduced, the algebraic dissipation rate model (57)–(59) still holds if the extended definition of $\overline{W}_{ij}$ is used:

$$\overline{W}^E_{ij} = \overline{W}_{ij} + \frac{7\alpha_3 + 12}{7\alpha_3 + 1}e_{mji}\Omega_m. \tag{79}$$

The definition of ξ given in (59) must then be replaced with $\xi \equiv (\overline{W}^E_{ij}\overline{W}^E_{ij})^{1/2}K/\varepsilon$. Non-inertial effects are then systematically accounted for in the algebraic dissipation rate model.

A few comments need to be made about the simplified near-equilibrium model (73)–(74). As shown by Speziale (1990), for any dissipation rate model of the form (73), $C^*_{\varepsilon 1} = 1$ constitutes a bifurcation point. For turbulent flows that are far from equilibrium (particularly, when $\eta \gg 1$), the simplified model (73) has the capability of rendering values of $C^*_{\varepsilon 1}$ that are close to 1 when $C_{\varepsilon 1} = 1$. Consequently, when used with a two-equation model, it may be advisable to raise the value of $C_{\varepsilon 1}$ in (73)–(74) to a value greater than 1.15 (we have used values as large as 1.20). With this adjusted value, acceptable equilibrium results for benchmark turbulent flows are still obtained and potential problems in non-equilibrium situations are avoided by staying sufficiently far away from the bifurcation point. There are no such difficulties with the complete algebraic dissipation rate model given by (57) and (68) where we can set $C_{\varepsilon 1} = 1$.

5. Illustrative tests and comparisons

We will first show results for the new dissipation rate model corresponding to the problem of homogeneous shear flow in a rotating frame (see figure 1). This problem is chosen since it encapsulates the stabilizing or destabilizing effect of a system rotation

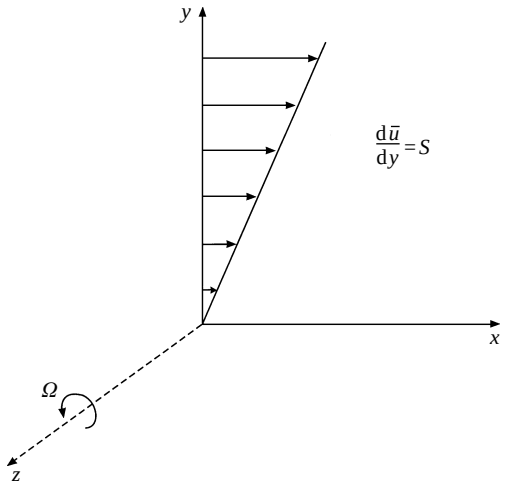

FIGURE 1. Schematic of homogeneous shear flow in a rotating frame.

on basic shear flow, unencumbered by the complicating features of turbulent diffusion and wall blocking. At time $t = 0$, an initially isotropic turbulence is subjected to a uniform shear rate S and a system rotation Ω specified by

$$\frac{\partial \overline{v}_i}{\partial x_j} = \begin{pmatrix} 0 & S & 0 \\ 0 & 0 & 0 \\ 0 & 0 & 0 \end{pmatrix}, \quad \Omega_i = (0, 0, \Omega) \tag{80}$$

where S and Ω are constants. Due to the isotropic initial conditions, $(b_{ij})_0$ and $(d_{ij})_0$ are initially zero, where a subscript 0 denotes the initial value. The solution then only depends on SK_0/ε_0 and Ω/S. In the limit as $\Omega \to 0$, we have pure homogeneous shear flow and, in the limit as $S \to 0$, we have isotropic turbulence in a rotating frame.

In figure 2(*a–c*), we show the time evolution of the turbulent kinetic energy for three different values of the ratio of rotation to shear rate: $\Omega/S = 0$, 0.25 and 0.5 (here, $K^* = K/K_0$ and $t^* = St$). The model calculations are all based on the Speziale *et al.* (1991) pressure–strain model (hereafter, referred to as the SSG model) which is given by

$$\begin{aligned} \Pi_{ij} = &-C_1 \varepsilon b_{ij} + C_2 \varepsilon \left(b_{ik} b_{kj} - \tfrac{1}{3} b_{kl} b_{kl} \delta_{ij} \right) \\ &+ C_3 K \overline{S}_{ij} + C_4 K \left(b_{ik} \overline{S}_{jk} + b_{jk} \overline{S}_{ik} - \tfrac{2}{3} b_{kl} \overline{S}_{kl} \delta_{ij} \right) + C_5 K (b_{ik} \overline{W}_{jk} + b_{jk} \overline{W}_{ik}) \end{aligned} \tag{81}$$

where

$$C_1 = 3.4 + 1.8 \mathscr{P}/\varepsilon, \quad C_2 = 4.2, \quad C_3 = \tfrac{4}{5} - 1.30 (b_{ij} b_{ij})^{1/2}, \quad C_4 = 1.25, \quad C_5 = 0.40. \tag{82}$$

Three sets of model results are displayed corresponding to the SSG model: one using the full tensor dissipation rate transport model (50), another using the complete algebraic dissipation rate model (57) with (68), and another based on the standard isotropic dissipation rate model (38) with $C_{\varepsilon 1} = 1.44$ and $C_{\varepsilon 2} = 1.83$. All of the model results are compared with the large-eddy simulations (LES) of Bardina, Ferziger & Reynolds (1983) for an initial condition of $SK_0/\varepsilon_0 = 3.38$. From figure 2(*a*) for pure shear flow ($\Omega/S = 0$), it appears that the full tensor dissipation rate transport model only yields a minor improvement to the isotropic dissipation rate transport model. The important point is that the algebraic dissipation rate model yields a reasonably

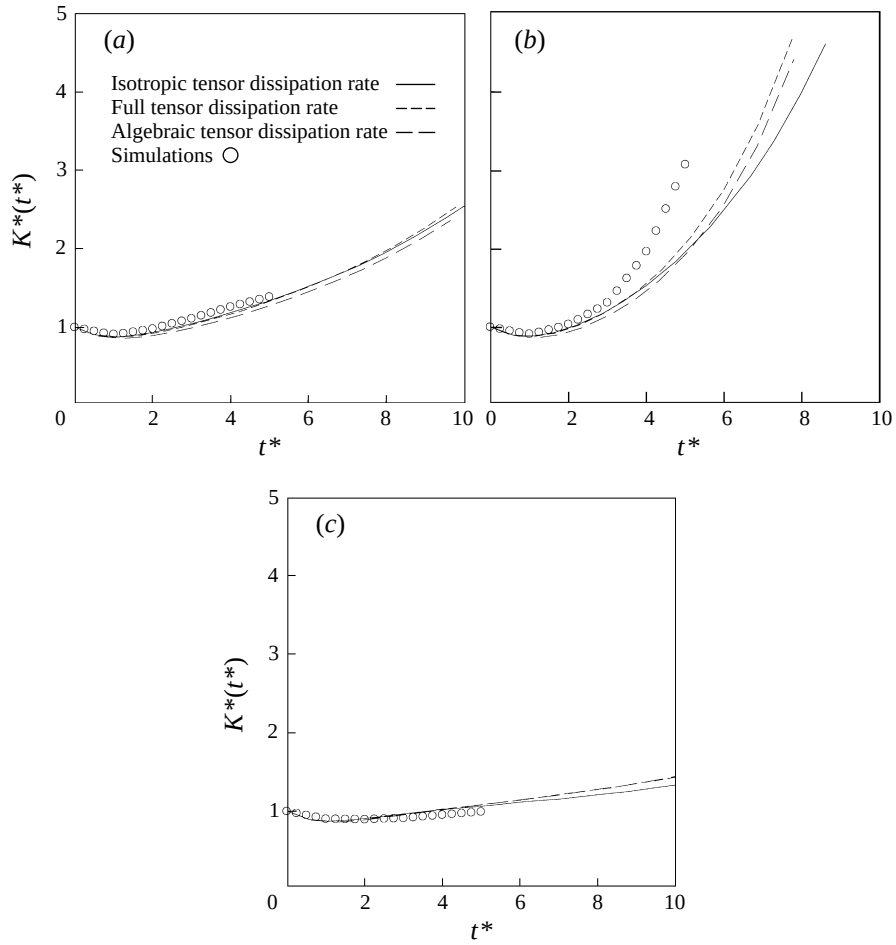

FIGURE 2. Time evolution of the turbulent kinetic energy for homogeneous shear flow in a rotating frame: comparison of the model predictions with the large-eddy simulations of Bardina *et al.* (1983). (*a*) $\Omega/S = 0$, (*b*) $\Omega/S = 0.25$ and (*c*) $\Omega/S = 0.5$.

good approximation to the full tensor dissipation rate transport model. The same is true of the $\Omega/S = 0.25$ and $\Omega/S = 0.5$ cases shown in figures 2(*b*) and 2(*c*). It is encouraging to note that the $\Omega/S = 0.25$ case is better represented by the anisotropic dissipation rate model. While virtually all second-order closures underpredict the growth rate of this highly energetic case, the addition of anisotropic dissipation leads to a considerable improvement as shown in figure 2(*b*) and places the most energetic state, by far, at $\Omega/S = 0.25$ as mentioned earlier.

In figure 3(*a,b*), composites of the LES, anisotropic dissipation rate model, and IP model predictions for rotating homogeneous shear flow are shown for $\Omega/S = 0$, 0.25 and 0.5. It is clear from these composite results that the new algebraic anisotropic dissipation rate model does an excellent job in capturing the trends of the LES whereas the IP model does poorly. One notable feature about these results is the fact that, with the anisotropic dissipation rate model, equilibrium values of $\mathscr{P}/\varepsilon$ are predicted that depend on Ω/S. The new anisotropic dissipation rate model predicts that when $\Omega/S = 0 : (\mathscr{P}/\varepsilon)_\infty = 1.90$, when $\Omega/S = 0.25 : (\mathscr{P}/\varepsilon)_\infty = 3.64$, and when

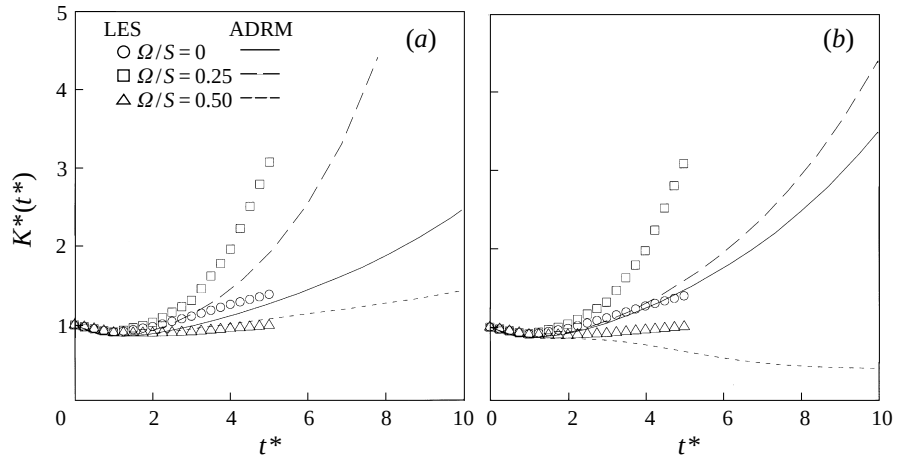

FIGURE 3. Composite of results for the time evolution of the turbulent kinetic energy in rotating homogeneous shear flow. (*a*) Large-eddy simulations (LES) of Bardina *et al.* (1983) and new anisotropic dissipation rate model (ADRM), and (*b*) LES and IP model.

$\Omega/S = 0.5 : (\mathscr{P}/\varepsilon)_\infty = 1.78$, where $(\cdot)_\infty$ denotes the equilibrium value obtained in the limit as $t \to \infty$. This is physically consistent since the model predicts the more energetic cases to have larger equilibrium values of $\mathscr{P}/\varepsilon$. On the other hand, any traditional second-order closure with the standard isotropic dissipation rate model (38) erroneously predicts a universal equilibrium value of (see Speziale 1990)

$$\left(\frac{\mathscr{P}}{\varepsilon}\right)_\infty = \frac{C_{\varepsilon 2} - 1}{C_{\varepsilon 1} - 1} \tag{83}$$

for any homogeneous turbulent flow. While the specific quantitative comparisons for rotating homogeneous shear flow may only appear to constitute a modest improvement when anisotropic dissipation is added to the SSG model (see figure 2) they constitute a major improvement over the commonly used IP model with isotropic dissipation as can be seen from figure 3(*b*). We provide results of the IP model as a benchmark since this model is so widely used. The IP model is a simplified version of the Launder *et al.* (1975) pressure–strain model which is a special case of (81) for which $C_1 = 3.6$, $C_2 = 0$, $C_3 = 4/5$ and $C_4 = C_5 = 1.20$; it is solved along with (38) wherein $C_{\varepsilon 1} = 1.44$ and $C_{\varepsilon 2} = 1.90$. It is clear from figure 3(*b*) that the IP model prematurely restabilizes (at $\Omega/S \approx 0.37$) and does not respond properly to changes in the rotation rate. This illustrates the relative importance of using the proper pressure–strain model.

The new anisotropic dissipation rate model was compared with the same range of homogeneous turbulence DNS results from Speziale *et al.* (1991) and Speziale, Gatski and Sarkar (1992). The new model, in most cases, yielded only modest improvements over the standard SSG model with isotropic dissipation. One notable exception was the C128U DNS case of Rogers *et al.* (1986) for homogeneous shear flow. (This particular DNS case was chosen because it is the best resolved of the group studied by Rogers, private communication.) Here the, addition of the anisotropic dissipation rate model led to a significant improvement over the predictions of the SSG and IP models with isotropic dissipation. This can be seen clearly in figure 4(*a*,*b*) for the time evolution of the turbulent kinetic energy and scalar dissipation rate.

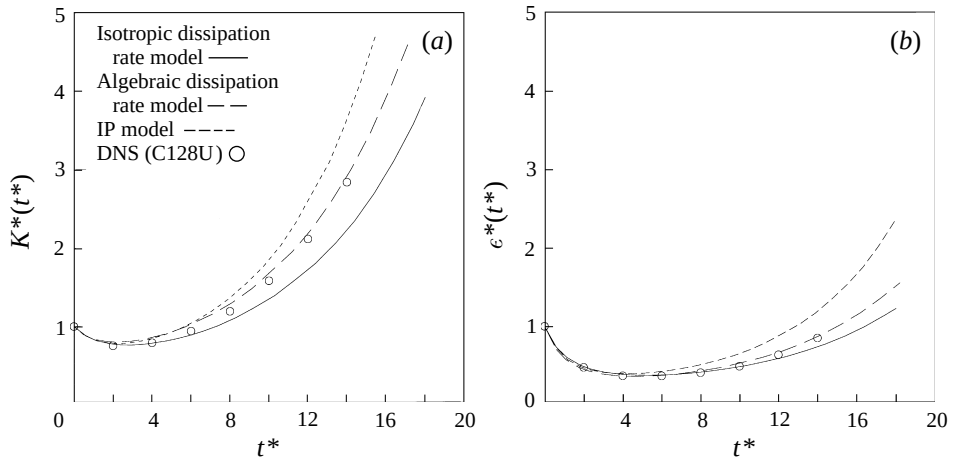

FIGURE 4. Comparison of the model predictions with the DNS results of Rogers *et al.* (1986) for homogeneous shear flow. (*a*) Turbulent kinetic energy and (*b*) turbulent dissipation rate.

Equilibrium values	ADRM model	IP model	DNS
b_{11}	0.216	0.190	0.215
b_{12}	−0.159	−0.185	−0.158
b_{22}	−0.139	−0.095	−0.153
b_{33}	−0.082	−0.095	−0.062
SK/ε	5.98	5.42	5.70

TABLE 2. Equilibrium values for homogeneous shear flow: comparison of the new anisotropic dissipation rate model (ADRM) with the IP model and with the DNS of Rogers *et al.* (1986).

Equilibrium values	ADRM model	IP model	Experimental data
b_{11}	0.198	0.148	0.22
b_{12}	−0.153	−0.170	−0.16
b_{22}	−0.122	−0.074	−0.15
b_{33}	−0.077	−0.074	−0.07
SK/ε	3.27	2.95	3.1

TABLE 3. Equilibrium values for the logarithmic region of a turbulent boundary layer: comparison of the new anisotropic dissipation rate model (ADRM) with the IP model and with the mean experimental data of Laufer (1951) from channel flow.

In table 2, the equilibrium values for homogeneous shear flow predicted by the new algebraic anisotropic dissipation rate model (ADRM) are compared with the DNS results of Rogers *et al.* (1986). In table 3, the results predicted by the new anisotropic dissipation rate model for the logarithmic region of an equilibrium turbulent boundary layer (where $\mathscr{P}/\varepsilon = 1$) are compared with experiments. It is clear that these results are excellent in comparison to the IP model whose results are also displayed to provide a benchmark as mentioned earlier (the results, however, only constitute a mild improvement over those obtained from the SSG model with isotropic dissipation as indicated earlier; also see Speziale *et al.* 1991). Since the equilibrium turbulent

boundary layer forms a cornerstone for many engineering calculations, it is important to do well here. The new model does so and without wall reflection terms (see Abid & Speziale 1993).

At this point, some comments are in order concerning how the new model compares with previous proposals. Most previously proposed algebraic models for d_{ij} have been parameterized in terms of the Reynolds stress anisotropy tensor in the form

$$d_{ij} = C_{d1}\varepsilon b_{ij} + C_{d2}\varepsilon\left(b_{ik}b_{kj} - \tfrac{1}{3}b_{kl}b_{kl}\delta_{ij}\right) \tag{84}$$

where C_{d1} and C_{d2} are either constants or functions of the invariants of b_{ij} (see Lumley 1978 and Hallbäck *et al.* 1990). When models of this kind have been used, they have tended to be solved with the same scalar dissipation rate equation (38) that applies when anisotropies in the dissipation rate are neglected – an obvious inconsistency. As shown by the analysis presented herein, there should be a nonlinear dependence on the mean velocity gradients that is different than that for the Reynolds stress tensor in equilibrium (the reader should compare the coefficients of (57) and (70)). Obviously, due to some nonlinear scrambling, the mean velocity gradients do not imprint the same anisotropy on the large and small scales.

A variety of empirical models have been proposed over the years where the dissipation rate is modelled as

$$\dot{\varepsilon} = C_{\varepsilon 1}\frac{\varepsilon}{K}\mathscr{P} - C^{*}_{\varepsilon 2}\frac{\varepsilon^2}{K} \tag{85}$$

where $C^{*}_{\varepsilon 2}$ is a function of the mean velocity gradients. Models of the form (85) can be converted to the form (73) by the introduction of a suitable dependence of $C^{*}_{\varepsilon 1}$ on $\mathscr{P}/\varepsilon$. Pope (1978) proposed a model that is equivalent to (85) with

$$C^{*}_{\varepsilon 2} = 1.92 - 0.79\overline{S}_{ij}\overline{W}_{jk}\overline{W}_{ki}\frac{K^3}{\varepsilon^3} \tag{86}$$

in an effort to resolve the round jet/plane jet anomaly. However, this mean velocity gradient correction to $C^{*}_{\varepsilon 2}$ vanishes in two-dimensional mean turbulent flows, thus rendering no correction to the benchmark flows considered in this study. Furthermore, there is an additional problem with this proposal. The commonly used dissipation rate equation (38) – as well as the modifications proposed herein – guarantee that $\varepsilon = 0$ is a fixed point (i.e. when ε vanishes, $\dot{\varepsilon}$ also vanishes). This is crucial to guarantee at least limited realizability, namely positive values for the turbulent kinetic energy and dissipation rate in all homogeneous flows (see Speziale 1990). The Pope (1978) proposal violates this fixed point constraint and therefore can yield unrealizable results for the turbulent kinetic energy and dissipation rate in homogeneous turbulence. Such basic violations of realizability are almost always computationally fatal.

The Hanjalic & Launder (1980) modification is also of the form (85) with

$$C^{*}_{\varepsilon 2} = 1.92 + 0.27\frac{K^2}{\varepsilon^2}e_{mij}e_{mkl}\frac{\partial\overline{v}_i}{\partial x_j}\frac{\partial\overline{v}_k}{\partial x_l} \tag{87}$$

and, as with the Pope correction, $C_{\varepsilon 1} = 1.44$. Since

$$\frac{\partial\overline{v}_i}{\partial x_j} = \overline{S}_{ij} + \overline{W}_{ij}$$

it follows that the Hanjalic & Launder (1980) correction can be written in the form

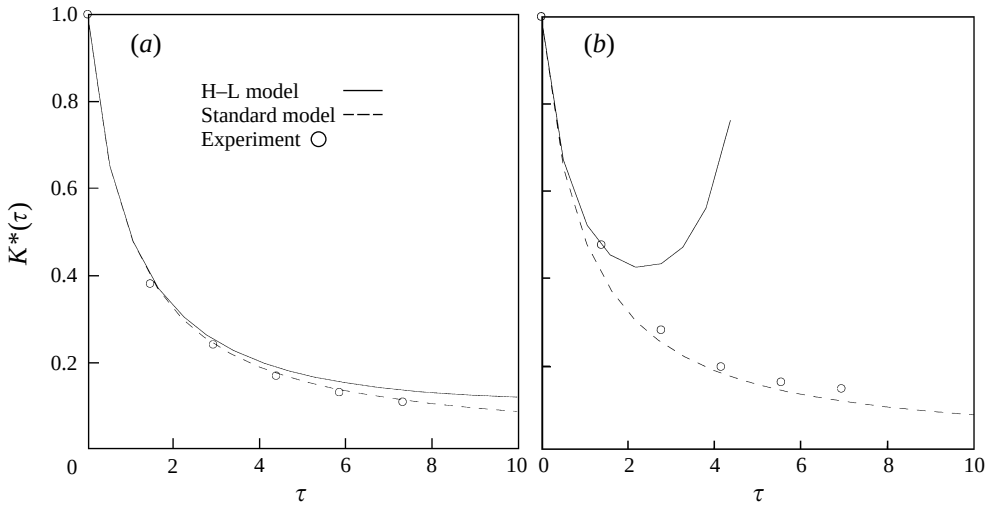

FIGURE 5. Decay of turbulent kinetic energy in rotating isotropic turbulence: comparison of the Hanjalic & Launder (1980) (H-L) model with the standard model and with the experiments of Wigeland & Nagib (1978). (*a*) $\Omega K_0/\varepsilon_0 = 0.123$ and (*b*) $\Omega K_0/\varepsilon_0 = 0.469$.

(73); for near equilibrium turbulent flows where (71) applies it takes the form

$$C^*_{\varepsilon 1} = 1.44 - 0.27\frac{\xi^2}{C^*_\mu \eta^2} \tag{88}$$

with $C_{\varepsilon 2} = 1.92$. For consistency, the absolute mean vorticity tensor (78) must be used in the definition of ξ in non-inertial frames. Calculations for the two limits of rotating homogeneous shear flow – namely, for $S = 0$ and $\Omega = 0$ – are revealing. The former case ($S = 0$) corresponds to isotropic turbulence in a rotating frame. In figure 5(*a*), the decay of turbulent kinetic energy in rotating isotropic turbulence predicted by the Hanjalic & Launder model is compared with the predictions of the standard model (38), where $C_{\varepsilon 1} = 1.44$ and $C_{\varepsilon 2} = 1.92$, and with the experimental data of Wigeland & Nagib (1978) for $\Omega K_0/\varepsilon_0 = 0.123$. In this figure, $K^* = K/K_0$ and $\tau = \varepsilon_0 t/K_0$. It is clear from these results that the Hanjalic & Launder model reacts too strongly to this weak rotation, predicting a reduction in the decay rate that is overly large. In figure 5(*b*), the same comparisons are made for the stronger rotation rate of $\Omega K_0/\varepsilon_0 = 0.469$. This rotation rate causes a modest reduction in the decay rate that cannot be predicted by the standard model which ignores rotation. However, the Hanjalic & Launder model predicts too strong a reduction in the decay rate for $\tau \leqslant 2$; then the model becomes unrealizable when $\tau \approx 4$ (it predicts a negative dissipation rate which is computationally fatal). The problem with realizability becomes clear when one analyses the dissipation rate equation associated with the Hanjalic & Launder model which can be written in the form

$$\dot{\varepsilon} = 1.44\frac{\varepsilon}{K}\mathscr{P} - 1.92\frac{\varepsilon^2}{K} - 0.27K\overline{\omega}_i\overline{\omega}_i \tag{89}$$

where $\overline{\omega}_i = e_{ijk}\partial\overline{v}_k/\partial x_j + 2\Omega_i$ is the absolute mean vorticity. Unlike the standard model, the Hanjalic & Launder modification allows for the possibility that $\dot{\varepsilon} < 0$ when $\varepsilon = 0$ – a mathematical feature that can lead to serious violations of realizability through the development of negative dissipation rates. The reduction in the decay rate of isotropic

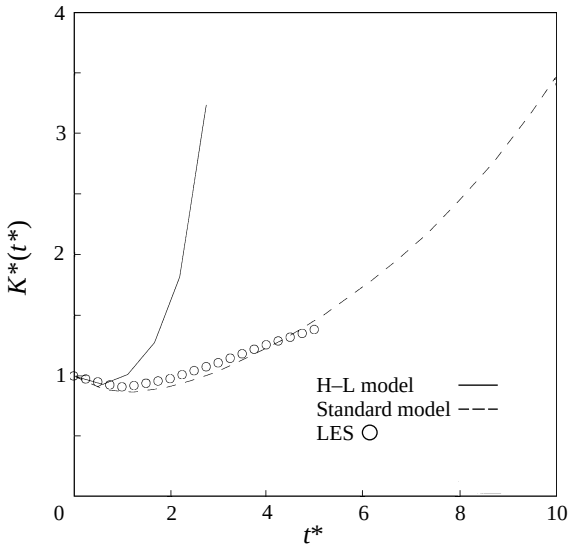

FIGURE 6. Time evolution of the turbulent kinetic energy in homogeneous shear flow: comparison of the predictions of the Hanjalic & Launder (1980) model with the standard model and with the large-eddy simulation of Bardina *et al.* (1983).

turbulence from a system rotation results from a non-equilibrium effect whereby (64) breaks down (see Mansour, Cambon & Speziale 1991). It cannot be properly modelled by *ad hoc* rotational corrections to the coefficient $C_{\varepsilon 2}$. In figure 6, the Hanjalic & Launder (1980) model is compared with the standard dissipation rate model – as well as with the LES results of Bardina *et al.* (1983) – in homogeneous shear flow ($\Omega = 0,\ S > 0$). From these results it is obvious that the Hanjalic & Launder model has a growth rate that is far too large. The application of a discernible rotation rate makes the model unrealizable. It is thus clear that the introduction of an *ad hoc* functional dependence on the mean velocity gradients in the coefficient $C_{\varepsilon 2}$ can cause serious problems.

Now, we will present two more challenging applications involving inhomogeneous turbulent flows – one of which is wall bounded. To be specific, we have considered the spatially evolving turbulent plane wake as well as turbulent flow in a square duct. We will consider the latter flow first, which is fully developed corresponding to a Reynolds number $Re = 4800$ based on the duct width and centreline mean velocity. Due to the fact that the Reynolds number of the DNS is somewhat low, we will only be able to make qualitative comparisons (simulations of the companion problem of turbulent channel flow have tended to indicate that the qualitative features of the flow are quite similar between high and low Reynolds number cases). In figure 7(*a*), we display the secondary flow pattern in a square duct (for one quadrant of the duct) obtained from the DNS of Gavrilakis (1992) for a Reynolds number $Re = 4800$ (also see Mompean *et al.* 1996). The corresponding secondary flow pattern obtained from the SSG second-order closure with the new algebraic anisotropic dissipation rate model (ADRM) is displayed in figure 7(*b*). As is evident from these results, the qualitative agreement is quite good. On the other hand, when the SSG second-order closure is applied to this flow with the standard isotropic dissipation rate model, the results are not so favourable as shown in figure 7(*c*). With isotropic dissipation, the SSG model erroneously predicts the presence of enhanced secondary flow cells

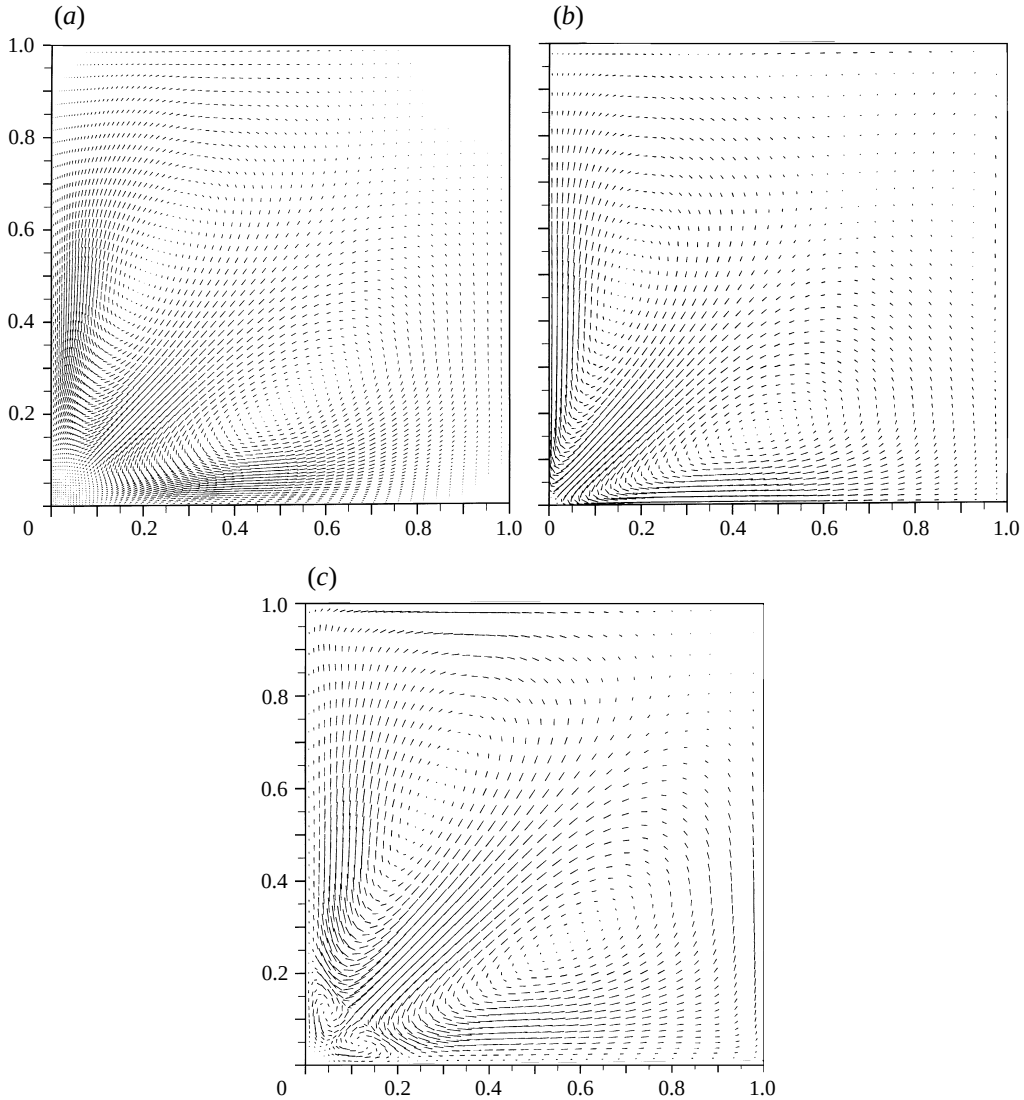

FIGURE 7. Computed secondary flow pattern in a square duct ($Re = 4800$): (*a*) DNS of Gavrilakis (1992), (*b*) SSG model with ADRM, and (*c*) SSG model with isotropic dissipation (calculations by G. Mompean).

near the duct corner which are not supported by DNS. These results were obtained with the variable-$C^*_{\varepsilon 1}$ formulation of the ADRM given by (57) and (73)–(74) with the inhomogeneous generalization (77); the integration was performed with wall functions to avoid the ambiguities associated with near-wall modelling.

In order to provide some more detailed quantitative comparisons, we considered the spatially evolving flat-plate turbulent wake that was measured recently by Marasli, Champagne & Wygnanski (1991). This is at a Reynolds number $Re_\theta \approx 1000$ based on the momentum thickness where the measurements were taken far enough downstream to ensure complete self-similarity. In figure 8, results for the turbulent kinetic energy profiles in the far-field wake are displayed that were computed by Cimbala (1995). Here, we compare the predicted results for the SSG model – with anisotropic as well

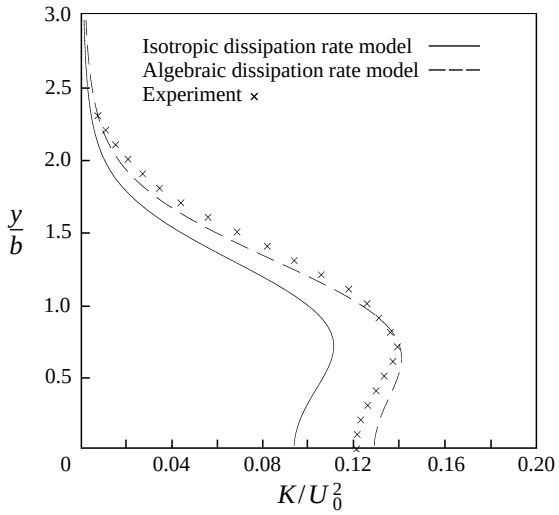

FIGURE 8. Comparison of the SSG model predictions with the experiments of Marasli *et al.* (1991) for the turbulent kinetic energy profiles in the turbulent plane wake (calculations by J. M. Cimbala).

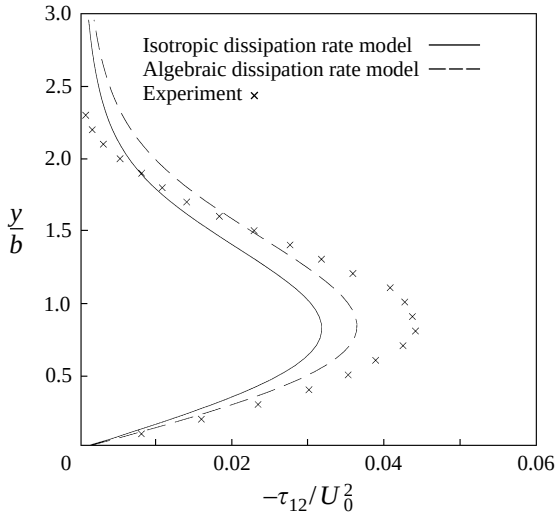

FIGURE 9. Comparison of the SSG model predictions with the experiments of Marasli *et al.* (1991) for the Reynolds shear stress profiles in the turbulent plane wake (calculations by J. M. Cimbala).

as isotropic dissipation – with the far-field wake measurements of Marasli *et al.* (1991). It is clear from these results that the inclusion of the new anisotropic dissipation rate model leads to a considerable improvement. The same is true of the corresponding Reynolds shear stress profiles that are provided in figure 9 (see Cimbala 1995). Again all of these results were obtained with the variable-$C^*_{\varepsilon 1}$ formulation of the ADRM given by (57), (73)–(74) with the inhomogeneous generalization (77).

Finally, it should be noted that recently some isotropic dissipation rate models of the form (73) have been proposed where $C^*_{\varepsilon 1} = C^*_{\varepsilon 1}(\eta)$. Yakhot *et al.* (1992) developed an RNG-based $K - \varepsilon$ model with a dissipation rate transport equation of the form

(73) where

$$C_{\varepsilon 1}^{*} = 1.42 - \frac{\eta(1-\eta/\eta_0)}{1+\beta\eta^3} \tag{90}$$

and η_0 and β are constants. The specific form of (90) was arrived at via a heuristic Padé approximation. This model has been shown to outperform the standard $K-\varepsilon$ model of Launder & Spalding (1974) in flows involving vortex shedding and separation. Lumley (1992) proposed a dissipation rate model that depends on the history of η; for near equilibrium turbulent flows that model is equivalent to (73) with

$$C_{\varepsilon 1}^{*} \propto 1/\eta. \tag{91}$$

While these models are interesting, they do not rigorously account for the effects of anisotropic dissipation which lead to a dependence on rotational as well as irrotational strain rates through each of the invariants η and ξ as shown herein.

6. Conclusion

A new model for the anisotropy of dissipation has been developed based on a systematic analysis of the transport equation for the dissipation rate tensor ε_{ij}. The transport equation for ε_{ij} was closed for homogeneous turbulent flows based on tensor symmetry properties combined with scaling arguments and the assumption that anisotropies in the dissipation rate are relatively small. Then, by invoking the same equilibrium hypothesis that gives rise to algebraic stress models of turbulence, an algebraic model for the anisotropy of dissipation was extracted from the transport equation for ε_{ij} by the use of integrity bases methods. This model differs from all previously proposed models in two notable ways:

(i) The anisotropy of dissipation depends explicitly on the mean velocity gradients in a nonlinear fashion, calling into question the commonly adopted practice of combining the deviatoric part of the dissipation rate tensor with traditional pressure–strain models which are linear in these terms as provided in (14).

(ii) This anisotropy gives rise to a scalar dissipation rate equation where the production of dissipation depends nonlinearly on the invariants of both rotational and irrotational strain rates.

The new algebraic dissipation rate model was tested in homogeneous turbulence and in the logarithmic region of an equilibrium turbulent boundary layer as well as in two non-trivial inhomogeneous turbulent flows. All of the results obtained were quite encouraging. Most notably, when the anisotropy of dissipation is accounted for, equilibrium values for the ratio of production to dissipation are predicted that depend on how the flow is strained. The traditionally used model – which neglects anisotropies in the dissipation rate – erroneously predicts a universal equilibrium value for the ratio of production to dissipation in all strained homogeneous turbulent flows.

While previous dissipation rate models have been proposed which introduce additional nonlinear terms that depend on the invariants of the mean velocity gradients, this is the first such model to be systematically derived (as shown in §5, *ad hoc* models along these lines can be ill-behaved). In our opinion, an algebraic model for the anisotropy of dissipation has reasonably good prospects for success since the dissipation tends to equilibrate on a fast time scale. The alternative is to solve the full ε_{ij} transport equation (50) with the addition of turbulent diffusion terms. However, since this substantially increases the level of computation required – and presents

problems in providing boundary conditions for each component of the dissipation rate tensor – we feel that this approach is debatable. Nonetheless, future research can be pursued along these lines as has recently been done by Oberlack (1995) in an interesting study. Further tests and refinements of this new algebraic dissipation rate model are envisaged for the future. This initiative towards the more systematic analysis and modelling of the dissipation rate tensor is a worthwhile effort that has too often been neglected and warrants much future research.

The first author (C.G.S.) acknowledges the support of the Office of Naval Research under Grant N00014-94-1-0088 (*ARI on Nonequilibrium Turbulence*, Dr L. P. Purtell, Program Officer). Partial support was also provided by the National Aeronautics and Space Administration under NASA Contract No. NAS1-19480 while the first author was in residence at ICASE. The authors are indebted to Dr M. M. Rogers (NASA Ames Research Center) for providing us with his DNS data for the dissipation rate tensor in homogeneous shear flow. Thanks are also due to Dr J. M. Cimbala (The Pennsylvania State University) and Dr G. Mompean (Swiss Federal Institute of Technology) for providing us with their calculations of the far wake and square duct.

Appendix

Equation (55) constitutes a linear system of algebraic equations for the determination of d_{ij}. This implicit system has an explicit solution of the form

$$d_{ij} = d_{ij}(\overline{\boldsymbol{S}}, \overline{\boldsymbol{W}}) \tag{A1}$$

with a parametric dependence on the ratio of production to dissipation, $\mathscr{P}/\varepsilon$. This dependence is expected to be a polynomial due to the linearity of the system. The most general polynomial representation of the form (A1) is given by

$$\boldsymbol{d} = \sum_{\lambda} G^{(\lambda)} \boldsymbol{T}^{(\lambda)} \tag{A2}$$

where $\boldsymbol{T}^{(\lambda)}$ are the integrity bases. For two-dimensional mean velocity gradients $\overline{\boldsymbol{S}}$ and $\overline{\boldsymbol{W}}$, there are *three* linearly independent integrity bases (see Pope 1975 and Gatski & Speziale 1993):

$$\boldsymbol{T}^{(1)} = \overline{\boldsymbol{S}}, \tag{A3}$$

$$\boldsymbol{T}^{(2)} = \overline{\boldsymbol{S}}\ \overline{\boldsymbol{W}} - \overline{\boldsymbol{W}}\ \overline{\boldsymbol{S}}, \tag{A4}$$

$$\boldsymbol{T}^{(3)} = \overline{\boldsymbol{S}}^2 - \tfrac{1}{3}\mathrm{tr}(\overline{\boldsymbol{S}}^2)\boldsymbol{I}, \tag{A5}$$

where $\boldsymbol{I}$ represents the unit tensor and tr$(\cdot)$ denotes the trace. The direct substitution of (A2) into (55) leads to a linear system of the form

$$A^{(1)}\boldsymbol{T}^{(1)} + A^{(2)}\boldsymbol{T}^{(2)} + A^{(3)}\boldsymbol{T}^{(3)} = 0 \tag{A6}$$

where the coefficients $A^{(\lambda)}$ depend linearly on $G^{(\lambda)}$. This is arrived at after the Cayley–Hamilton theorem is invoked which implies that

$$\overline{\boldsymbol{S}}^3 + \mathrm{II}_{\overline{\boldsymbol{S}}}\overline{\boldsymbol{S}} = 0, \tag{A7}$$

$$\overline{\boldsymbol{W}}^3 + \mathrm{II}_{\overline{\boldsymbol{W}}}\overline{\boldsymbol{W}} = 0 \tag{A8}$$

for two-dimensional mean velocity gradients where II denotes the second invariant.

From (A6), it follows that

$$A^{(1)} = A^{(2)} = A^{(3)} = 0 \tag{A9}$$

due to the linear independence of the integrity bases. Equation (A9) provides a linear system of three simultaneous equations for the determination of $G^{(1)}$, $G^{(2)}$ and $G^{(3)}$. The substitution of the resulting expressions for $G^{(\lambda)}$ in (A2) leads to the representation (57) for d_{ij}.

REFERENCES

Abid, R. & Speziale, C. G. 1993 Predicting equilibrium states with Reynolds stress closures in channel flow and homogeneous shear flow. *Phys. Fluids* A **5**, 1776–1782.

Bardina, J., Ferziger, J. H. & Reynolds, W. C. 1983 Improved turbulence models based on large-eddy simulation of homogeneous, incompressible turbulent flows. *Stanford University Tech. Rep.* TF-19.

Cimbala, J. M. 1995 Direct numerical simulations and modelling of a spatially evolving turbulent wake. *Proc. Tenth Symp. on Turbulent Shear Flows*, Vol. 1, pp. 6.25–6.30. The Pennsylvania State University, State College, PA.

Comte-Bellot, G. & Corrsin, S. 1971 Simple Eulerian time correlation of full and narrow-band velocity signals in grid-generated isotropic turbulence. *J. Fluid Mech.* **48**, 273–337.

Durbin, P. A. & Speziale, C. G. 1991 Local anisotropy in strained turbulence at high Reynolds numbers. *Trans. ASME*: *J. Fluids Engng* **113**, 707–709.

Gatski, T. B. & Speziale, C. G. 1993 On explicit algebraic stress models for complex turbulent flows. *J. Fluid Mech.* **254**, 59–78.

Gavrilakis, S. 1992 Numerical simulation of low-Reynolds-number turbulent flow in a square duct. *J. Fluid Mech.* **244**, 101–129.

Hallbäck, M., Groth, J. & Johansson, A. V. 1990 An algebraic model for nonisotropic turbulent dissipation rate in Reynolds stress closures. *Phys. Fluids* A **2**, 1859–1866.

Hanjalic, K. & Launder, B. E. 1980 Sensitizing the dissipation equation to irrotational strains. *Trans. ASME*: *J. Fluids Engng* **102**, 34–40.

Hinze, J. O. 1975 *Turbulence*. McGraw-Hill.

Laufer, J. 1951 Investigation of turbulent flow in a two-dimensional channel. *NACA TN* 1053.

Launder, B. E., Reece, G. J. & Rodi, W. 1975 Progress in the development of a Reynolds stress turbulence closure. *J. Fluid Mech.* **68**, 537–566.

Launder, B. E. & Spalding, D. B. 1974 The numerical computation of turbulent flows. *Comput. Methods Appl. Mech. Engng* **3**, 269–289.

Lee, M. J. & Reynolds, W. C. 1985 Numerical experiments on the structure of homogeneous turbulence. *Stanford University Tech. Rep.* TF-24.

Lumley, J. L. 1978 Computational modelling of Turbulent Flows. *Adv. Appl. Mech.* **18**, 123–176.

Lumley, J. L. 1992 Some comments on turbulence. *Phys. Fluids* A **4**, 203–211.

Mansour, N. N., Cambon, C. & Speziale, C. G. 1991 Single point modelling of initially isotropic turbulence under uniform rotation. *Annual Research Briefs - 1991, Center for Turbulence Research*, pp. 159–167, Stanford University Press.

Marasli, B., Champagne, F. & Wygnanski, I. 1991 On linear evolution of unstable disturbances in a plane turbulent wake. *Phys. Fluids* A **3**, 665–674.

Maréchal, J. 1972 Etude experimentale de la déformation plane d'une turbulence homogéne. *J. Méc.* **11**, 263–294.

Mompean, G., Gavrilakis, S., Machiels, L. & Deville, M. O. 1996 On predicting the turbulence-induced secondary flows using nonlinear $K-\varepsilon$ models. *Phys. Fluids* **8**, 1856–1868.

Oberlack, M. 1995 Non-isotropic dissipation in non-homogeneous turbulence. *J. Fluid Mech.* submitted.

Pope, S. B. 1975 A more general effective viscosity hypothesis. *J. Fluid Mech.* **72**, 331–340.

Pope, S. B. 1978 An explanation of the turbulent round jet/plane jet anomaly. *AIAA J.* **16**, 279–281.

Reynolds, W. C. 1987 Fundamentals of turbulence for turbulence modelling and simulation. *Lecture Notes for Von Kármán Institute, AGARD Lecture Series 86*. NATO.

Rogallo, R. S. 1981 Numerical experiments in homogeneous turbulence. *NASA TM*-81315.

Rogers, M. M., Moin, P. & Reynolds, W. C. 1986 The structure and modelling of the hydrodynamic and passive scalar fields in homogeneous turbulent shear flow. *Stanford University Tech. Rep.* TF-25.

Saddoughi, S. G. & Veeravalli, S. V. 1994 Local isotropy in turbulent boundary layers at high Reynolds number. *J. Fluid Mech.* **268**, 333–372.

Speziale, C. G. 1990 Turbulence modelling: present and future. *Lecture Notes in Physics*, vol. 357, pp. 490–512. Springer.

Speziale, C. G. 1991 Analytical methods for the development of Reynolds stress closures in turbulence. *Ann. Rev. Fluid Mech.* **23**, 107–157.

Speziale, C. G. 1996 Modelling of turbulent transport equations. In *Modelling and Simulation of Turbulent Flows* (ed. T. B. Gatski, M. Y. Hussaini & J. L. Lumley), pp. 185–242. Oxford University Press.

Speziale, C. G. & Bernard, P. S. 1992 The energy decay in self-preserving isotropic turbulence revisited. *J. Fluid Mech.* **241**, 645–667.

Speziale, C. G., Gatski, T. B. & Sarkar, S. 1992 On testing models for the pressure–strain correlation of turbulence using direct simulations. *Phys. Fluids* A **4**, 2887–2899.

Speziale, C. G., Sarkar, S. & Gatski, T. B. 1991 Modelling the pressure–strain correlation of turbulence: an invariant dynamical systems approach. *J. Fluid Mech.* **227**, 245–272.

Sreenivasan, K. R. 1991 On local isotropy of passive scalars in turbulent shear flows. *Proc. R. Soc. Lond.* A **434**, 165–182.

Tavoularis, S. & Corrsin, S. 1981 Experiments in nearly homogeneous turbulent shear flow with a uniform mean temperature gradient. Part 1. *J. Fluid Mech.* **104**, 311–347.

Wigeland, R. A. & Nagib, H. M. 1978 Grid-generated turbulence with and without rotation about the streamwise direction. *Illinois Institute of Technology Fluids and Heat Transfer Rep.* R78-1.

Yakhot, V., Orszag, S. A., Thangam, S., Gatski, T. B. & Speziale, C. G. 1992 Development of turbulence models for shear flows by a double expansion technique. *Phys. Fluids* A **4**, 1510–1520.